Journal of Materials Chemistry A

PAPER



Cite this: J. Mater. Chem. A, 2017, 5, 13098

# Continuous microfiber drawing by interfacial charge complexation between anionic cellulose nanofibers and cationic chitosan†

Rafael Grande, Eliane Trovatti, Antonio J. F. Carvalho* and Alessandro Gandini

Received 20th March 2017
Accepted 22nd May 2017

DOI: 10.1039/c7ta02467c

rsc.li/materials-a

This study describes a novel process of drawing fibers generated by the electrostatic complexation of negatively charged nanocellulose fibers with positively charged chitosan macromolecules. The process involves the continuous pulling of the aqueous media incorporating each polymer at their interface. The morphology of the wet and dry fibers, assessed by optical and electron microscopy, shows that the cellulose nanofibers surrounded by chitosan were aligned along the fiber direction. This was supported by the very high mechanical properties of the dry fibers.

## Introduction

The electrostatic interaction between polymers bearing opposite charges has given rise to a comprehensive realm of materials, which find applications in a variety of important domains,[1] including layer-by-layer (LbL) architectures[2–4] and polyionic complexes (PIC).[5–9] The possibility of generating fibers which incorporate such ionic interactions has also been studied.[10] Among the numerous charged polymers investigated, chitosan, a renewable macromolecule readily prepared from natural chitin, represents a very interesting substrate because its primary amino groups can be readily protonized, whereby it becomes soluble in mildly acidic aqueous media.[11–14] The present study describes a novel approach within this general field, based on the association of cationic chitosan with negatively charged cellulose nanofibers. To the best of our knowledge, this strategy has never been described in the scientific literature, the closest approach to it being a study by Zou and Kim, who prepared fibers and other self-assembled structures from a suspension of negatively charged graphene oxide nanosheets in an aqueous cationic chitosan solution, using a pull-out process that induced the orientation of the nanosheets and hence a controlled morphology.[15] Regrettably, no mechanical characterization was carried out on these materials. The use of cellulose nanofibers could lead to a strong electrostatic binding between the two macromolecular components and an enhancement of the mechanical properties of the ensuing polyionic composite, given the well-known strength displayed by the different forms of nanocellulose, one of the remarkable features associated with these original and highly successful nanofibers derived from the most widespread renewable resource.[16–19]

Of the three classical nanocellulose morphologies, our choice fell onto the nanofibrilated form prepared in the presence of 2,2,6,6-tetramethylpiperidine-1-oxyl (TEMPO), a process that generates carboxylic moieties at their surface.[20,21] The obtained fibrils are hereafter denoted here as To-CNF. The oppositely charged chitosan was used as an acetic acid aqueous solution to ensure the conversion of its amino groups into the corresponding ammonium cations. In order to prepare the substrate from which the fibers were drawn, different proportions of the oppositely charged components were mixed in an aqueous medium in order to establish the best solution/suspension concentration ratio in relation to the properties of the final dry fibers.

## Experimental

### Materials

Surface-charged nanocellulose fibers were prepared from a sugarcane bagasse pulp fibre suspension (10 g, 2% wt), sodium bromide (1 mmol $g^{-1}$ cellulose) and 2,2,6,6-tetramethylpiperidine-1-oxyl (TEMPO) free-radical reagent (0.1 mmol $g^{-1}$ cellulose). Sodium bromide and TEMPO were added into the pulp suspension. Sodium hypochlorite (NaClO) (5 mmol $g^{-1}$ cellulose) was slowly added to the fiber suspension and then the pH was adjusted to 10 by adding 0.1 M NaOH. The mixture was stirred for 6 h at room temperature. The resulting cellulose pulp was washed with deionized water up to neutral pH and then sonicated using a high power ultrasonicator (22 kHz, 400 W) until the formation of a transparent gel. The carboxylic functions formed by the oxidation of the primary OH groups at the surface of the cellulose nanofibers were determined by conductometric titration and gave 1.8 mmol $g^{-1}$ (Fig. S1†). The final concentration of the To-CNF

University of São Paulo, Av. João Dagnone 1100, CEP, São Carlos, SP, Brazil. E-mail: toni@sc.usp.br

† Electronic supplementary information (ESI) available. See DOI: 10.1039/c7ta02467c

suspension was 0.15 wt% and the fiber width was about 25 nm, as can be seen in the ESI (Fig. S2†). The chitosan (pharmaceutical grade, $M_w$ 60.000 g mol$^{-1}$, deacetylation degree 89.5%) solution was prepared by dissolving 1 g of chitosan in 100 mL of 1% (v/v) aqueous acetic acid solution (pH 4).

### Fiber preparation

The fiber drawing was performed manually using precision tweezers. Droplets (100 μL) of the To-CNF suspension and of the chitosan solution were placed in contact on a Teflon plate. The visually observed ensuing interface was the locus in which the tweezers were carefully plunged to start the fiber drawing. The fibers were then dried at room temperature and wound on a reel.

### Merging two or more fibers

The individual fibers were merged together in an attempt to study the morphology of the resulting larger fiber. For this, two or more wet fibers were placed in contact just after their preparation.

### Fiber characterization

SEM images of the chitosan/To-CNF fibers were obtained using a FEI Inspect F50 electron microscope. All samples were sputter coated with platinum. Fractured sections were obtained in liquid nitrogen. Optical microscopy was performed immediately as the fiber was born from its pristine liquid medium using a Leica DM2700 microscope equipped with polarizer filters. FTIR spectra were acquired using a Perkin-Elmer Spectrum 100 FT-IR Spectrometer equipped with a single horizontal Golden Gate ATR cell from 32 scans with a resolution of 4 cm$^{-1}$. A PerkinElmer Pyris 1 TGA was performed to determine decomposition patterns and insights into the fiber composition. Temperature scans were performed from 25 to 800 °C, with a heating rate of 10 °C min$^{-1}$ under a nitrogen atmosphere. Elemental analysis (CNH) was also performed on a Perkin Elmer 2400 series II to obtain more accurate results about the fiber composition. The tensile strength of the fibers was obtained using a Perkin-Elmer DMA 800 dynamic mechanical analyzer working in tension mode at 1 Hz, at room temperature. The fibers were conditioned for 24 h at 50% humidity at 22–24 °C, before the mechanical tests, which were carried out on 25 fiber samples prepared in different experiments.

## Results and discussion

The operational principle adopted to generate the fibers consisted in depositing a droplet (10–1000 μL) of the chitosan solution and that of the To-CNF suspension onto a Teflon surface in such a way that the two hemispherical drops would be in lateral contact. Thereafter precision tweezers were inserted at the interface (Fig. 1a) and gently pulled the viscous thread of the mixture (Fig. 1b), until the exhaustion of the available liquid (see ESI Video†). The wet thread was then allowed to dry spontaneously (Fig. 1c) to produce a thin fiber (Fig. 1d), whose properties were assessed.[15] It was anticipated that this modus operandi would induce the progressive alignment of the cellulose nanofibers and the chitosan macromolecules, thus

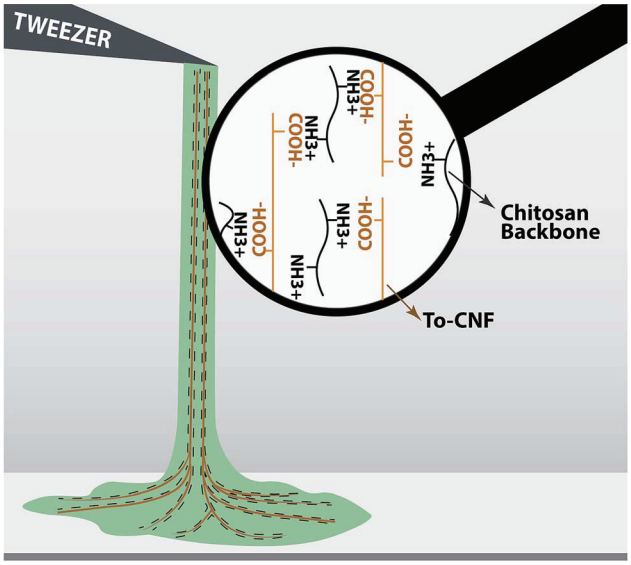


Fig. 2 Schematic view of the electrostatic interactions between the protonated chitosan and the anionic To-CNF during the wet-drawing fiber-forming process.

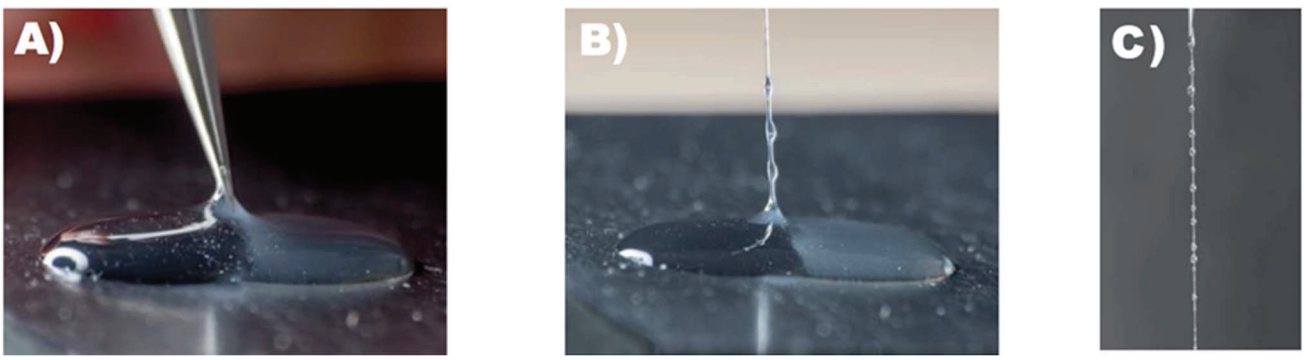


Fig. 1 (A) Formation of the interface between the To-CNF suspension (clear liquid) and chitosan solution (cloudy liquid), (B) gently pulling the viscous thread from the interface, and (C) fiber image taken immediately after wet-drawing.

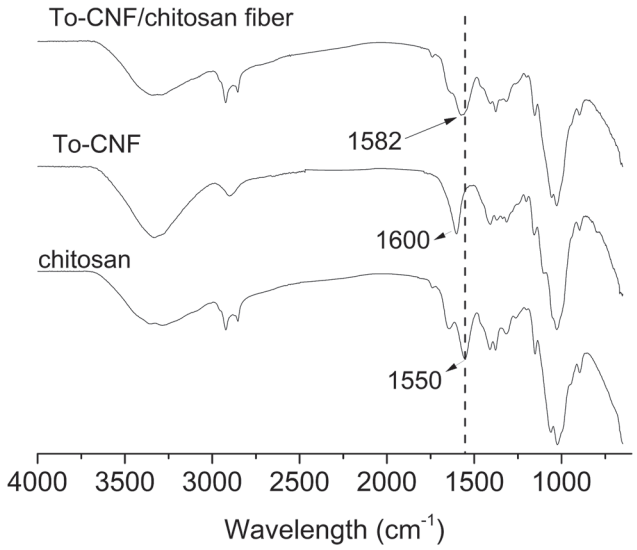


Fig. 3 FTIR spectra of chitosan, TEMPO modified cellulose nanofibers (To-CNF) and microfibers formed by To-CNF/chitosan complexation.

maximizing the reinforcement provided by To-CNFs. Fig. 2 depicts an idealized schematic view drawn with the purpose of illustrating these interactions, in which the chitosan macromolecules (here unrealistically too thick and too long) are fully stretched (an unlikely situation, although the extent of stretching was quite significant) and aligned with the nanocellulose fibers. It is important to emphasize that dipping the tweezers in either individual droplet did not produce any of the phenomenology described above, since pulling the liquid produced its immediate breakage (see ESI Video†). Furthermore, approaching a chitosan solution droplet to a water counterpart resulted in an immediate coalescence, which clearly indicated that the generation of a stable interface in our system was induced by the rapid formation of the electrostatic interionic complexation between the two oppositely charged polymers when the two droplets reached contact.

The regularly spaced droplets shown in Fig. 1c were formed by Plateau–Rayleigh instabilities.[22] The droplets were collected using a micropipette and analyzed by FTIR (Fig. S3†) showing

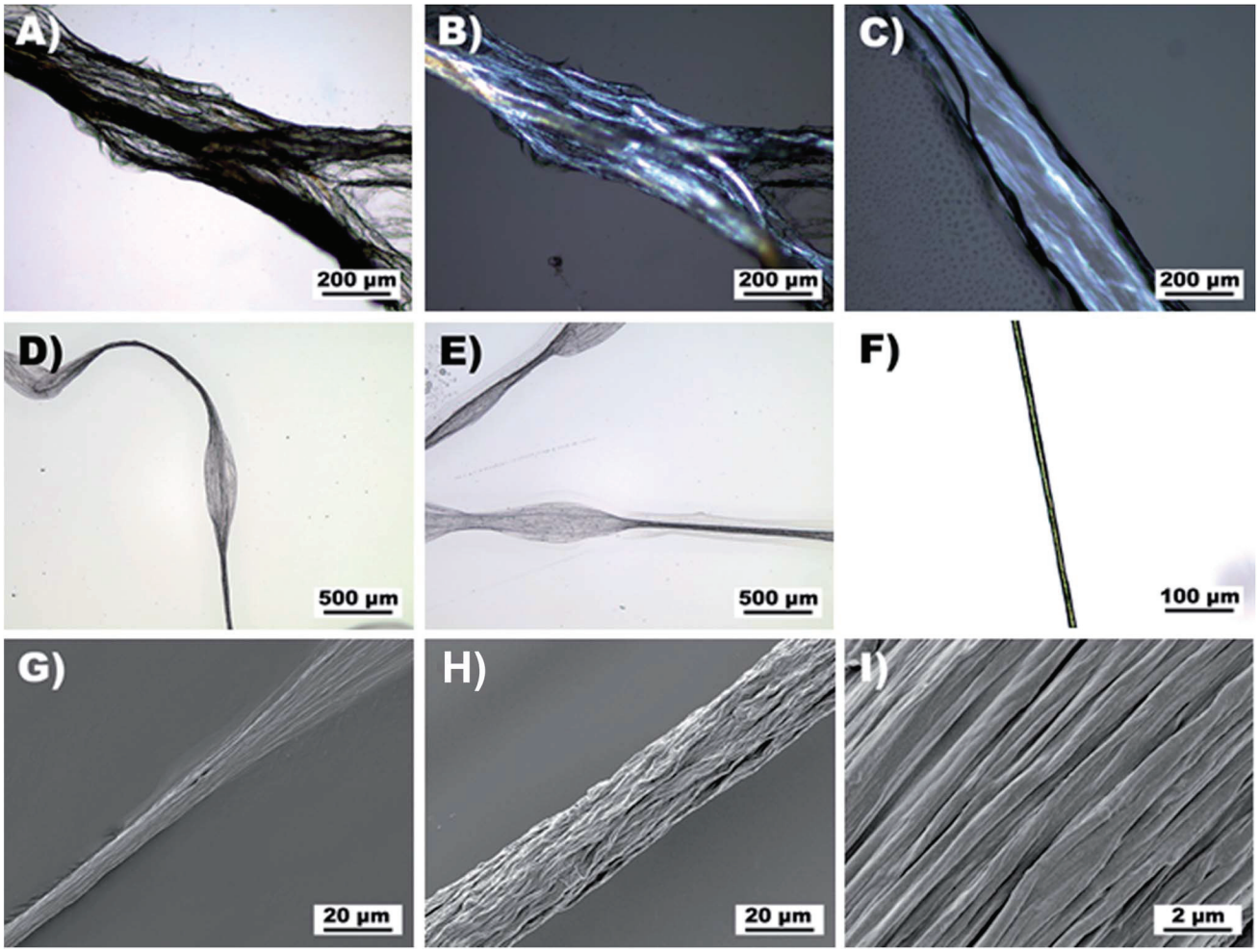


Fig. 4 Optical microscopy images of (A) the wet drawing in the transition zone from droplet to fiber in normal light and (B) polarized light, (C) wet fiber under polarized light, (D) the fibers immediately after being drawn from the liquid medium and in its early stage of drying (see exuded water), (E) the drying fiber, and (F) dried fiber. (G) SEM images of the transition zone from film to fiber showing a film composed of several embedded fibers aligned in the drawing direction; (H) the microfiber formed after drying and (I) its magnified surface showing fibrils regularly aligned along the microfiber direction.

 

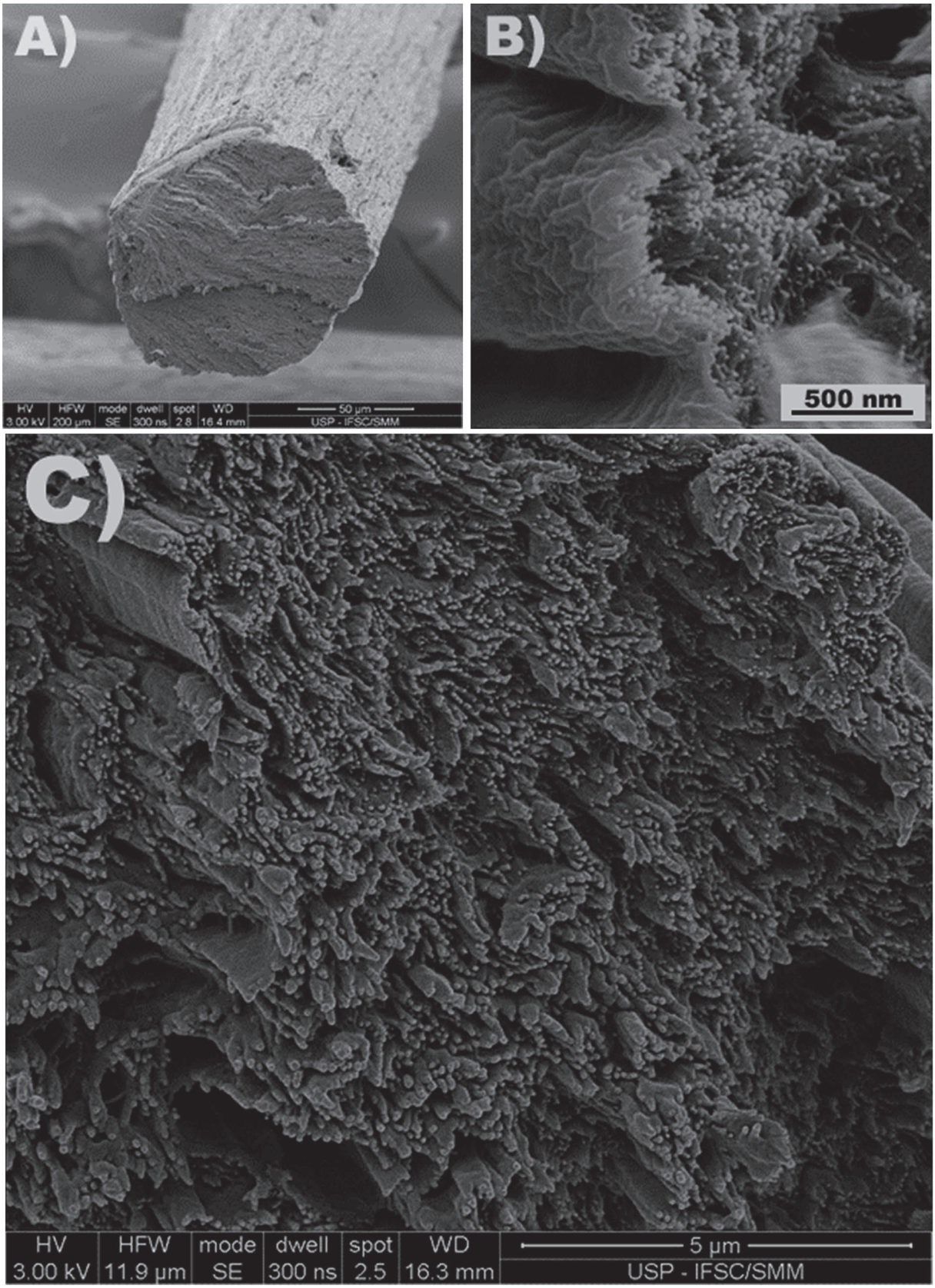


Fig. 5 SEM images of the fiber cross-section (A), showing (B) the edge of the fractured surface and (C) the middle area of the fractured fiber in which the nanofibers are aligned along the longitudinal axis.

that they were composed essentially of water, generated by the aqueous solvent expulsion while chitosan and To-CNF associated electrostatically to form the fiber.

The dry fibers were characterized by FTIR-ATR and TGA as well as optical and scanning electron microscopy, and mechanical properties. Their FTIR spectrum was compared with those of dry To-CNF and a dried sample of chitosan obtained from an acetic acid solution. The only significant difference was found in the 1500–1600 $cm^{-1}$ region, Fig. 3, where the To-CNF carboxylate peak at 1600 $cm^{-1}$ and the protonated chitosan $NH_3^+$ peak at 1550 $cm^{-1}$ merged into a new absorption peak at 1582 $cm^{-1}$ corroborating the formation of a donor–acceptor interionic complex between the two polysaccharides.[23] The TGA thermograms showed the degradation pattern typical of a mixture containing essentially To-CNF (Fig. S4†). More accurate composition of the fibers was obtained *via* elemental analysis which revealed that the fibers are composed of about 87% To-CNF and 13% chitosan, corroborating TGA curves.

Fig. 4 shows typical images of fibers taken by optical and electron microscopy. The evolution of the fiber morphology is illustrated by the sequence of images, including those taken under polarized light, from Fig. 4a and b (progressive fiber assembly in the aqueous medium) to Fig. 4c (newly born fiber) to Fig. 4d and e (process of water expulsion) and Fig. 4f (dried fiber). This sequence provided two important observations, namely the bundle-type assembly within the nascent fiber and the orientation of the nanocellulose threads, as seen in the birefringent images. These indications were supported by the SEM images, where Fig. 4g shows a fiber which was forcibly dried while being generated, and Fig. 4h and i depict a regularly dried fiber at two different magnifications, the higher resolution clearly showing the bundling of fibrillar structures of about 500 nm diameter, aligned in the 20 μm thick fiber direction.

SEM images of the cross-section of the chitosan/To-CNF fibers, obtained by fracturing them in liquid nitrogen, are shown in Fig. 5. The surfaces revealed a sharp and a compact structure (Fig. 5a) formed by dense fibril bundles (Fig. 5b) and continuous folded layers (Fig. 5c). This morphology suggests that the To-CNF nanofibers, whose diameter ranged from 25 to 75 nm, had been covered by a sleeve of chitosan during the fiber formation thanks to the ionic associations, giving rise to the observed bundles and that the continuous layers were made up of higher amounts of chitosan, well-known for its film-forming ability. The other important feature here is the very good alignment of the sleeved cellulose nanofibers in the direction of the drawing process, which corroborates the schematic representation shown in Fig. 2.

Measurements of the fiber diameter, taken along several portions of each given fiber (generally with length of meters), showed a remarkable regularity, which was attributed to the fact that the drawing operation from the drop interface was a continuous process that maintained a constant surface area for the nascent wet fiber.

The wet fibers could be readily merged, as shown in Fig. 6 for two (Fig. 6a), four (Fig. 6b) or eight (Fig. 6c) single fibers, giving rise to correspondingly thicker homogeneous counterparts, which were obtained by simply placing the wet fibers in contact with each other along their longitudinal axis. Partial merging along this axis was also possible, resulting in branched morphologies, as in Fig. 6d and e. In other words, several types of fibrous architectures could be prepared by these straightforward operations followed by drying.

Another interesting feature of this system is associated with the combination of the fiber stiffness and flexibility, as highlighted by the fact that the dried fibers could be twisted into yarns (Fig. 6f) or tied into knots (Fig. 6g).

In order to determine the mechanical properties of the fibers, tension tests were carried out using single fibers. A

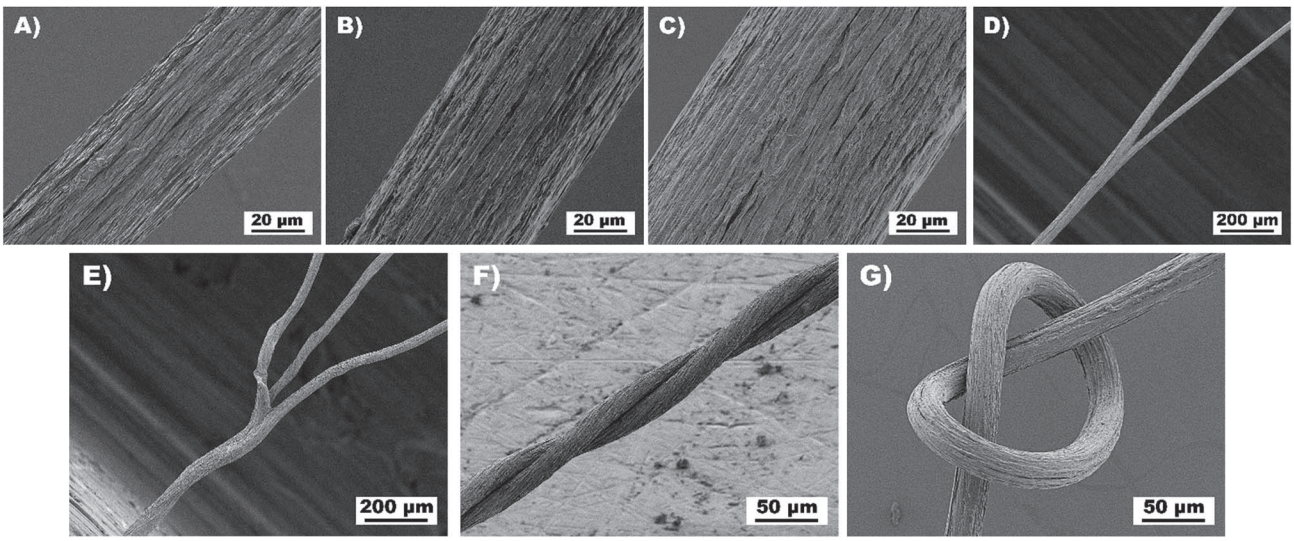


Fig. 6 SEM images of (A) two, (B) four and (C) eight completely merged fibers; (D and E) chitosan/To-CNF fibers partially merged generating brunched morphologies, (F) fibers twisted into a yarn, and (G) a fiber tied as a knot.

 

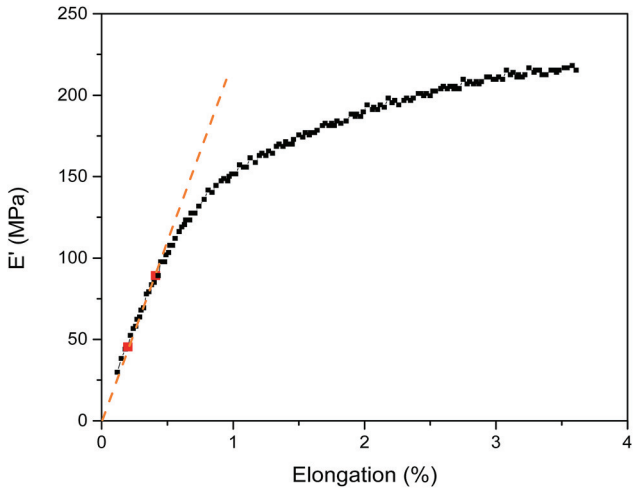


Fig. 7 Mechanical test on a single fiber, carried out by tension-mode DMA.

typical stress–strain curve accessed by DMA is shown in Fig. 7. The tensile modulus was about 22 GPa and the ultimate tensile strength, determined with a precision load cell, was 220 MPa. The tensile strength of these fibers reached values similar to those of cellulose nanofibers. The modulus was about double those of cellulose nanofibers, which are on average about 10 GPa,[16] including the mechanical properties from fibers obtained with highly oriented cellulose.[24] These high values are in tune with the fact that the chitosan-embedded To-CNF has a compact structure, as shown in the SEM images of Fig. 4 and 5.

## Conclusions

The mechanism put forward in this study represents a hitherto unexplored approach to the formation of continuous fibers of virtually any length and variable diameters through the electrostatic association between cationic macromolecule nanofibers as reinforcing elements, both components being derived from renewable resources. The growing interest in cellulose nanofibers finds here a novel working philosophy in which the top-down deconstruction process used to obtain them from conventional vegetable fibers is complemented by the bottom-up fiber drawing with an oppositely charged polymer in which they become imbedded in an orderly fashion, giving rise to remarkable mechanical properties.

Work is in progress to enlarge the scope of this strategy, including a comprehensive study of the role of the different process parameters, the fibers' sensitivity to moisture and surface modification, in view of establishing their most suitable applications.

## Acknowledgements

The authors acknowledge FAPESP for the post-doctoral fellowships of R. G. (2015/07744-0) and E. T. (2012/05184–0) and thank CNPq for PVE (401656/2013-6) of A. G. and for the 307124/2015-0 project. The authors also thank the Centro de Tecnologia de Materiais Híbridos (CTMH) of the Department of Materials Engineering, São Carlos School of Engineering, University of São Paulo, for the SEM facilities.

## References

1 A. P. Alberto Ciferri, *Ionic Interactions in Natural and Synthetic Macromolecules*, John Wiley & Sons, Hoboken, 2012.
2 G. Decher and J. B. Schlenoff, *Multilayer Thin Films*, Wiley-VCH Verlag GmbH & Co. KGaA, Weinheim, Germany, 2012, vol. 1–2.
3 S. Srivastava and N. A. Kotov, in *Semiconductor Nanocrystal Quantum Dots: Synthesis, Assembly, Spectroscopy and Applications*, 2008, pp. 197–216.
4 S. W. Keller, H. Kim and T. E. Mallouk, *J. Am. Chem. Soc.*, 1994, 8817–8818.
5 E. Tsuchida and K. Abe, in *Interactions Between Macromolecules in Solution and Intermacromolecular Complexes*, ed. E. Tsuchida and K. Abe, Springer-Verlag, Berlin/Heidelberg, 1982, pp. 1–119.
6 H. Yamamoto and Y. Senoo, *Macromol. Chem. Phys.*, 2000, **201**, 84–92.
7 H. Shen, T. Akagi and M. Akashi, *Chem. Lett.*, 2016, **45**, 220–222.
8 K. Ohkawa, Y. Takahashi, M. Yamada and H. Yamamoto, *Macromol. Mater. Eng.*, 2001, **286**, 168–175.
9 M. Amaike, Y. Senoo and H. Yamamoto, *Macromol. Rapid Commun.*, 1998, **19**, 287–289.
10 S. V. G. Nista, J. Bettini and L. H. I. Mei, *Carbohydr. Polym.*, 2015, **127**, 222–228.
11 M. Rinaudo, *Prog. Polym. Sci.*, 2006, **31**, 603–632.
12 M. N. Ravi Kumar, *React. Funct. Polym.*, 2000, **46**, 1–27.
13 C. K. S. Pillai, W. Paul and C. P. Sharma, *Prog. Polym. Sci.*, 2009, **34**, 641–678.
14 V. Zargar, M. Asghari and A. Dashti, *ChemBioEng Rev.*, 2015, **2**, 204–226.
15 J. Zou and F. Kim, *ACS Nano*, 2012, 121113102545003.
16 D. Klemm, F. Kramer, S. Moritz, T. Lindström, M. Ankerfors, D. Gray and A. Dorris, *Angew. Chem., Int. Ed.*, 2011, **50**, 5438–5466.
17 I. Siró and D. Plackett, *Cellulose*, 2010, **17**, 459–494.
18 N. Lavoine, I. Desloges, A. Dufresne and J. Bras, *Carbohydr. Polym.*, 2012, **90**, 735–764.
19 D. Klemm, B. Heublein, H.-P. Fink and A. Bohn, *Angew. Chem., Int. Ed.*, 2005, **44**, 3358–3393.
20 T. Saito, S. Kimura, Y. Nishiyama and A. Isogai, *Biomacromolecules*, 2007, **8**, 2485–2491.
21 A. Isogai, T. Saito and H. Fukuzumi, *Nanoscale*, 2011, **3**, 71–85.
22 P.-G. de Gennes, F. Brochard-Wyart and D. Quéré, *Capillarity and Wetting Phenomena*, Springer New York, New York, NY, 2004.
23 C. Rosca, M. I. Popa, G. Lisa and G. C. Chitanu, *Carbohydr. Polym.*, 2005, **62**, 35–41.
24 K. M. O. Håkansson, A. B. Fall, F. Lundell, S. Yu, C. Krywka, S. V. Roth, G. Santoro, M. Kvick, L. Prahl Wittberg, L. Wågberg and L. D. Söderberg, *Nat. Commun.*, 2014, **5**, 1–10.